CrossMark

Exploring how alternative mapping approaches influence fireshed assessment and human community exposure to wildfire

Joe H. Scott · Matthew P. Thompson ·
Julie W. Gilbertson-Day

Abstract Attaining fire-adapted human communities has become a key focus of collaborative planning on landscapes across the western United States and elsewhere. The coupling of fire simulation with GIS has expanded the analytical base to support such planning efforts, particularly through the "fireshed" concept that identifies areas where wildfires could ignite and reach a human community. Previous research has identified mismatches in scale between localized community wildfire planning and the broader fireshed considering patterns of wildfire activity across landscapes. Here we expand upon this work by investigating the degree to which alternative geospatial characterizations of human communities could influence assessment of community exposure and characterization of the fireshed. We use three methods of mapping human communities (point, raster, and polygon) and develop three fireshed metrics (size, number of fires reaching houses, and number of houses exposed), and apply this analytical framework on a 2.3 million ha case study landscape encompassing the Sierra National Forest in California, USA. We simulated fire occurrence and growth using FSim for 10,000 iterations (fire seasons) at 180-m resolution. The simulation resulted in 3.9 large fires per million ha per year, with a mean size of 3432 ha. Results exhibit similarities and differences in how exposure is quantified, specifically indicating that polygons representing recognized community boundaries led to the lowest exposure levels. These results highlight how choice of the mapping approach could lead to misestimating the scope of the problem or targeting mitigation efforts in the wrong areas, and underscore the importance of clarity and spatial fidelity in geospatial data representing communities at risk.

Keywords Wildland–urban interface · Fire-adapted community · Wildfire risk · Fireshed

Introduction

Wildfires in the wildland–urban interface (WUI) pose a significant threat to human communities, requiring assessment and planning to support risk mitigation and adaptation efforts (Calkin et al. 2014; Moritz et al. 2014; Williams 2013). Increased sophistication of spatial fire spread models, risk analysis techniques, and decision support systems (Pacheco et al. 2015; Thompson and Calkin 2011; Thompson et al. 2015a) has in turn led to increased sophistication of risk-based WUI assessments in fire-prone areas (e.g., Alcasena et al. 2015; Cova et al. 2013; Dennison et al. 2007; Haas et al. 2013; Kalabokidis et al. 2015; Mitsopoulos

J. H. Scott · J. W. Gilbertson-Day
Pyrologix, LLC, Missoula, MT, USA

M. P. Thompson (✉)
US Forest Service, Missoula, MT, USA
e-mail: mpthompson02@fs.fed.us

et al. 2015). Beyond identifying areas where flammable vegetation coincides with human development, a key feature of many of these assessments is the use of fire modeling and GIS to explore how fire weather and landscape conditions influence community exposure to wildfire. Consideration of landscape-scale patterns of fire occurrence and spread can significantly expand the requisite spatial scale of risk mitigation planning relative to typical scales of localized community wildfire protection planning (Williams et al. 2012).

An emerging thread of wildfire exposure and risk analysis is the notion of risk transmission across landscapes and the spatial identification of sources of exposure and risk (Ager et al. 2014a, b). In this context, exposure relates to the spatial overlap of potential wildfire activity within and adjacent to human communities, while risk further incorporates some measure of the effects or consequences of human community exposure to wildfire (Thompson and Calkin 2011). These analyses explore how the ignition location and the size, shape, and location of simulated fires influence patterns of exposure and potential loss. Scott et al. (2012), for instance, modeled the growth of unsuppressed wildfires that ignited on the Bridger-Teton National Forest (Wyoming, USA) in order to quantify the expected annual number of fires reaching the WUI and the expected annual WUI area burned. Similarly, Haas et al. (2015) merged simulated fire perimeters with population density metrics to identify locations along the Front Range of Colorado, USA, where ignitions could lead to the highest impacts to human communities.

A particularly useful transmission-based concept for wildfire planning is the biophysical fireshed, which is a delineated area within which ignitions can reach a resource or asset of interest such as designated critical habitat, a municipal watershed, or a human community (Thompson et al. 2013; Thompson et al. 2015b). Identifying the scale of potential exposure and risk transmission can help land managers and homeowners identify optimal strategies for co-managing risk and creating fire-adapted human communities (Ager et al. 2015). From a modeling perspective, the size, shape, and location of simulated fire perimeters will exert critical influence on the geographic extent of the biophysical fireshed, and these factors have been the primary focus of analyses to date.

However, the size, shape, and location of the human community—the focal point of the fireshed—will also

Fig. 1 Overview of the study area–Sierra National Forest, Fire ▶ Occurrence Area (FOA), and fire modeling extent. Simulated fires originated within the FOA but could spread to any portion of the fire modeling extent

influence fireshed delineation. Human communities are geospatially represented in three main ways: individual structure locations using point data, generalized structure locations using raster data, and community boundaries delineated with polygons (Calkin et al. 2011; Haas et al. 2013; Radeloff et al. 2005). To our knowledge, the degree to which alternative geospatial characterizations of human communities could influence assessment of the scale of risk transmission to communities and fireshed delineation has not been studied.
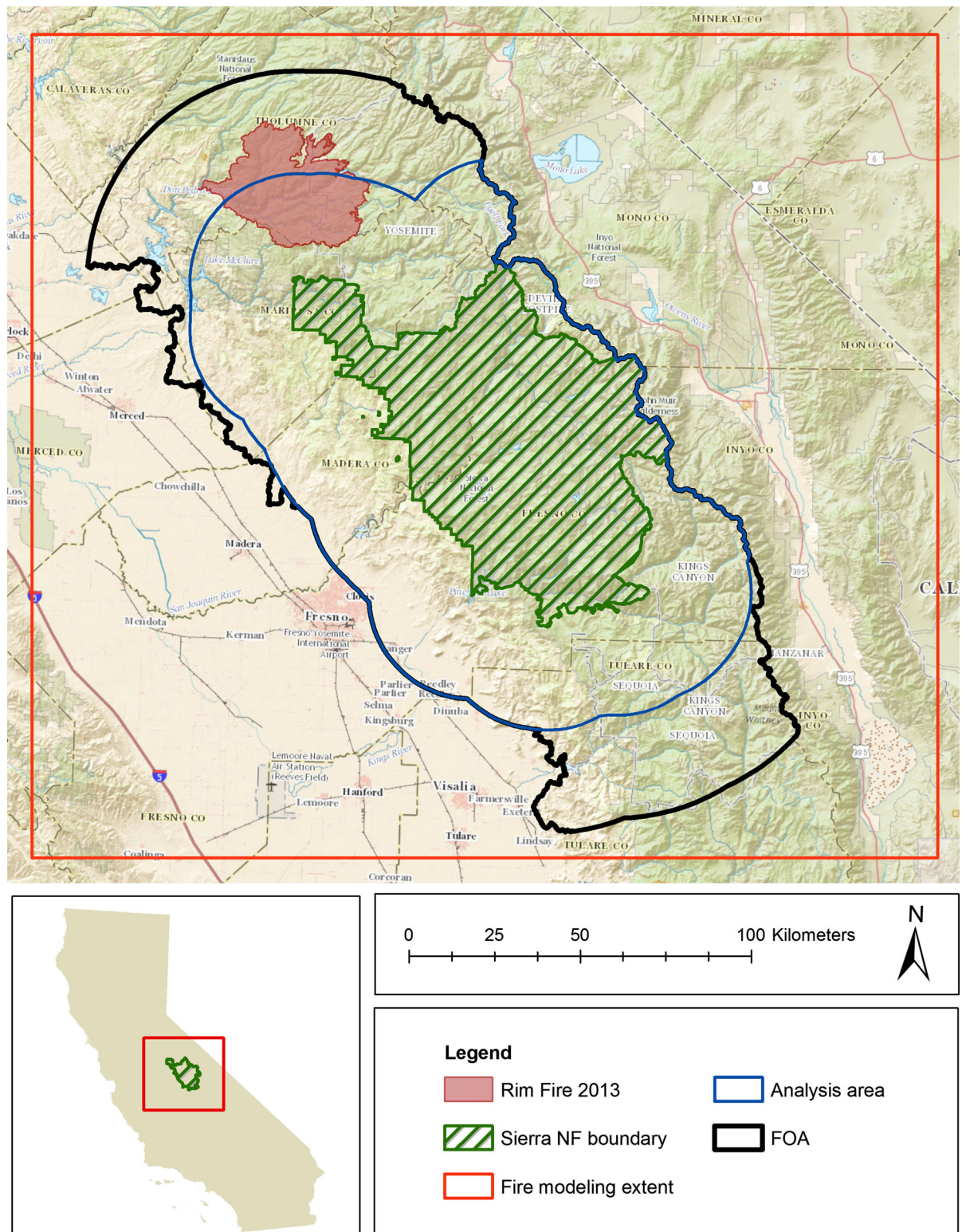
In this paper we leverage the fireshed concept to explore how raster, polygon and point methods of defining human communities influence calculations of exposure to wildfire. As a case study we apply stochastic wildfire simulation to a landscape containing the Sierra National Forest in California, USA. We develop three main fireshed metrics—size, number of fires reaching houses, and number of houses exposed—and illustrate how they vary with human community mapping method. We further compare exposure-source maps and probabilistic representations of number of houses exposed per simulated fire and fire season. The ultimate aim of this study is to yield insights and actionable information to support risk-informed community wildfire protection planning.

Methods

Study area

The 2.3 million ha study area consists of the Sierra National Forest and surrounding land ownerships, located on the western slope of the southern Sierra Nevada Mountains, California (Fig. 1). The eastern edge of the study area is the Sierra Crest at nearly 4000 m elevation. The Rim Fire of 2013 (114,008 ha)—the third largest wildfire in California's history—burned in the northern portion of this study area (Fig. 1).

Vegetation and topography vary widely across the study area. The extreme western portion of the study area consists of urban and agricultural land in the Central Valley. To the east and slightly higher in

Legend

Rim Fire 2013

Sierra NF boundary

Fire modeling extent

Analysis area

FOA

0   25   50   100 Kilometers

N

elevation, non-native annual grasslands dominate the base of the foothills. Chamise chaparral (*Adenostoma fasciculatum*) and mixed chaparral (including, *Quercus*, *Ceanothus* and *Arctostaphylos* species) are found in the foothills. The chaparral mixes with foothill woodlands populated with foothill pine (*Pinus sabiniana*) and blue oak (*Quercus douglasii*). A mixed-conifer forest, consisting primarily of ponderosa pine (*Pinus ponderosa*), sugar pine (*Pinus lambertiana*), incense cedar (*Libocedrus decurrens*), Douglas-fir (*Pseudotsuga menziesii*), dominates the mid elevations of the western slope of the Sierra. Forests dominated by white fir (*Abies concolor*) mixed with species from the mixed-conifer forest, and red fir (*Abies magnifica*) mixed with lodgepole pine (*Pinus contorta*) are found above the mixed-conifer forests. Finally, forests of lodgepole pine, limber pine (*Pinus flexilis*), whitebark pine (*Pinus albicaulis*) and foxtail pine (*Pinus balfouriana*) are found near timberline in the eastern portion of the study area.

Wildfire simulation

We used the FSim large-fire simulator (Finney et al. 2011) to generate a large-fire event set—a set of thousands of simulated wildfire perimeters that collectively represent a complete set of possible large-fire events, each with known probability of occurrence (Scott and Thompson 2015). FSim is a comprehensive wildfire occurrence, growth and suppression simulation system that pairs a wildfire growth model (Finney 1998, 2002) and a model of large-fire ignition probability with simulated weather streams in order to simulate wildfire occurrence and growth for thousands of fire seasons.

We used two of FSim's outputs in this study—a raster of burn probability (BP) and polygons, in ESRI Shapefile format, representing the final perimeter of each simulated wildfire. BP for a pixel is calculated as the number of times the pixel burned divided by the number of simulation iterations. FSim produces an annual BP result because an iteration represents a whole fire season. An attribute table specifying certain characteristics of each simulated wildfire—its start location and date, duration, final size, and other characteristics—is included with the shapefile. Fires occurring during the same simulated fire season are identified through attributes assigned to each fire so that the total area burned during an entire fire season

can be produced as well as individual-fire results. Fire intensity (flame-length class) that occurred within a perimeter is not recorded.

We used FSim to simulate 10,000 fire seasons at 180-m resolution, using the Scott and Reinhardt (2001) crown fire modeling method. The number and duration of simulated wildfires are not direct inputs to the model, but instead are the result of the simulation of weather and large-fire occurrence based on historical data. FSim requires a number of additional spatial and tabular inputs, described below.

Fire modeling landscape

Among FSim's spatial inputs is a fire modeling landscape file (LCP)—a raster representation of surface fuel (Scott and Burgan 2005), canopy fuel (canopy base height and canopy bulk density), forest vegetation (canopy cover and stand height) and topography (slope, aspect and elevation) across the fire simulation area. We used LANDFIRE version 1.3.0 (also known as "LANDFIRE 2012"), in NAD83 UTM11N geographic projection, as the source for the LCP (Ryan and Opperman 2013). We resampled the data layers from their native 30-m grid cell resolution to a 180-m cell size using the nearest neighbor method, then assembled a 180-m cell size.

Historical large-fire occurrence data

For historical fire occurrence inputs we used the Short (2014) Fire Occurrence Database (FOD), second edition, which covers the 22-year period 1992–2013. When parameterizing and calibrating FSim, we are only interested in the relatively few "large" (or escaped) wildfires that account for the overwhelming majority (typically more than 90 %) of the total area burned (Strauss et al. 1989). We used a threshold of 100 ha (247 ac) to identify a large fire. A size threshold is necessary to both parameterize and calibrate FSim. FSim's algorithms and sub-model components are designed to simulate the relatively small number of fires that escape initial control efforts and become large, spreading for days to weeks, and even months.

Anthropogenic fires accounted for 73 % of the total area burned in the study area from 1992 to 2013. However, the relative proportion of anthropogenic to naturally ignited wildfires varied significantly across

the study area. In the foothills of the western portion of the study area anthropogenic wildfires accounted for more than 95 % of the area burned. In the mountainous eastern portion of the study area, which has relatively little human influence, natural ignitions were responsible for more than 75 % of the area burned.

Historical weather data

FSim requires three weather-related inputs: monthly distributions of wind speed and direction, live and dead fuel moisture content by year-round percentile of the Energy Release Component variable of the National Fire Danger Rating System (NFDRS; citation) for fuel model G (*ERC-G*) class, and seasonal trend (daily) in the mean and standard deviation of *ERC-G*. We used two data sources for these weather inputs. For the wind speed and direction distributions we used the hourly (1200–2000 h) 10-min average values recorded at the Trimmer RAWS (NWS ID#044510) for the period 1990–2012. For ERC we sampled from a spatial dataset derived from North American Regional Reanalysis (NARR) 4-km *ERC-G* dataset for the period 1992–2012 (M. Jolly, Ecologist, personal communication).

The majority of large-fire area burned (90 %) occurs with fires that ignite between late June and mid-September. During that time, the 10-min average wind speeds (6.1-m above ground) are rarely greater than 20 km/h (as measured at the Trimmer remote automated weather station). At the trimmer RAWS, winds are southwest, west and northwest 70 % of the time during the large-fire season. Fine dead fuel moisture content during the large-fire season varied across the study area from a low of 2–3 % for exposed fuel at low elevations during periods of very dry weather (ERC-G > 97th percentile, to highs of 6–9 % for sheltered fuel at higher elevations during moderately dry conditions (when ERC-G was between the 80th and 90th percentile).

FSim fire occurrence inputs

FSim requires an FDist input file that specifies three inputs: (1) logistic regression coefficients that relate the probability of a large-fire day to *ERC-G*, (2) *AcreFract*—the ratio of the Fire Occurrence Area (FOA) size used in the FOD to the FOA size within the landscape—and (3) the distribution of the number of large fires per large-fire day. The *AcreFract* input was used in early implementations of FSim to account for the lack of complete fire occurrence data across an LCP. Until publication of the Short (2014) FOD, it was common to have historical fire records for only a fraction of the fire modeling landscape, so a logistic regression model of fire occurrence would under-simulate occurrence for the whole landscape. *AcreFract* is an adjustment factor on the probability of a large-fire day to make up for this lack of data. If fire occurrence data were available for only half of the LCP, then *AcreFract* = 0.5, and FSim effectively doubles the number of simulated fires to make up for the effect of the missing data on the logistic regression coefficients.

The FOA—the area within which we simulated fire starts—includes a 60-km buffer around the National Forest to the north/northwest and south, and a 30-km buffer to the west. A buffer was not added to the east because the forest boundary at that location is the Sierra Crest, and fires do not traverse the boundary from the east to the west. Buffers are necessary to account for fires that ignite outside of but can spread into the study area; buffer sizes were informed by analyzing past fires in the area and also by our experience with FSim.

To generate the FDist inputs we selected from the FOD only those large fires (≥100 ha) that started within the FOA (Fig. 1) and then generated logistic regression coefficients that estimate the probability of a large-fire day in relation to *ERC-G* as sampled from the NARR 4-km *ERC-G* at the location of the Trimmer RAWS. The FOA size in the FOD is identical to the FOA on the landscape, so *AcreFract* = 1.0. We also tabulated a frequency distribution of the number of large fires that occurred on each large-fire day.

Based on the historical large-fire start locations archived in the FOD, we used the Kernel Density tool of ERSI ArcGIS (with a 30 km search neighborhood and a 2 km pixel size) to create an ignition density grid (IDG). FSim uses this IDG to locate simulated fires on the landscape, placing more wildfires where the density of historical large wildfires is higher. Because we wanted to simulate only fires starting within the FOA, we set the IDG value outside the FOA to 0 so that FSim would not start any fires there. Because our LCP is larger than the FOA, a simulated fire could spread outside the FOA without immediately encountering the edge of the LCP. This buffer outside of the

FOA is important for comparing the simulated fire-size distribution to the historical.

Model calibration

We began by first calibrating, to the extent possible, the simulated large-fire size distribution and mean large-fire size compared to the historical. We accomplished this fire-size calibration using a combination of inputs—rate-of-spread adjustment factors by fuel model, dead and live fuel moisture contents by fuel model and percentile *ERC-G* bin, and perimeter trimming factor. We did not limit the maximum size of simulated wildfires.

After calibrating the fire-size distribution, we then calibrated the annual number of large-fire occurrences. FSim's fire occurrence inputs (logistic regression coefficients) are designed to simulate the probability of a large-fire day in relation to historical *ERC-G*. However, there are two known biases in FSim that can result in an under-simulation of the number of large fires compared to historical. First, FSim only ignites its simulated fires at or above the 80th percentile *ERC-G*, whereas historically, some percentage of large fires may have started when the *ERC-G* was below the 80th percentile. Those historical fires are represented in the logistic regression coefficients but are missing from the simulation. Second, the fire occurrence module of FSim implicitly assumes that each simulated fire becomes a large fire, meaning that it grows to at least the large-fire threshold of 100 ha. In the simulations, some percentage of simulated fires does not reach this threshold fire size. Those fires, too, are missing from the simulation.

It is easy to overcome these biases using the *AcreFract* input. Modifying the default *AcreFract* by (1) the fraction of historical large fires that started above the 80th percentile *ERC-G* and (2) by the fraction of all simulated fires that reached the large-fire size threshold gives an adjusted *AcreFract* that de-biases the number of large fires in the simulation

$$AcreFract_{adjusted} = Acrefract_{default} * \frac{N_{Hist80}}{N_{HistAll}} \\ * \frac{N_{SimLarge}}{N_{SimAll}}$$

where N_{Hist80} is the number of historical large-fire days for which *ERC-G* was at or above the 80th percentile, $N_{HistAll}$ is the total number historical large-fire days, $N_{SimLarge}$ is the number of simulated fires that reached the large-fire threshold, and N_{SimAll} is the total number of simulated fires.

Characterizing the human community

We used three datasets to characterize the human community in the study area. The Westwide Wildfire Risk Assessment (WWRA) produced a Where People Live (WPL) raster that represents the density of houses (houses/km^2) at a native cell size of 30 m (Oregon Department of Forestry 2013). Each WPL pixel therefore covers 900 m^2, or 0.0009 km^2. We multiplied the WPL density value by 0.0009 to produce an estimate of the number of houses per 30-m pixel.

$$\frac{Houses}{pixel} = \frac{Houses}{km^2} * \frac{0.0009 \, km^2}{pixel}$$

WPL is based on the LandScan population database from the Oakridge National Laboratory. LandScan represents spatially distributed population counts by the 2010 U.S. Census within census blocks polygons based on advanced modeling approaches which incorporate remotely sensed data such as nighttime lights and high-resolution imagery, along with local spatial data (Oregon Department of Forestry 2013).

We then found polygons representing 37 recognized communities, according to the U.S. Census Bureau's Incorporated Places and Census Designated Places data layer (U.S. Census 2014), located wholly or partially within the study area. These places are cities, towns, or Census Designated Places which provided a delineated boundary of concentrated populations, but are not legally incorporated in the state (U.S. Census 2014). We clipped these community polygons to the study area boundary, and then extracted the adjusted WPL values raster generated above. By definition, "communities only" population counts will be less than the WPL dataset.

Finally, we obtained cadastral data (parcel centroids) for the study area for portions of Fresno, Madera, Mariposa, Tulare, and Tuolumne counties, collected as part of the Federal Geographic Data Committee cadastral subcommittee efforts to map parcel data for 11 western states for fire management purposes (Calkin et al. 2011). Each improved-parcel centroid was taken to represent a single house (though in actuality improvement value could be for more than one structure per parcel).

We then clipped each of the human community datasets to our analysis area, a 2.3 million ha area formed by the intersection of the FOA and a 30 km buffer around the Sierra National Forest (Fig. 2). Estimates of the total number of houses in the study area were surprisingly similar between the WPL and parcel-centroid representations of the human community, with 51,929 houses represented in the WPL dataset and 51,155 houses based on the parcel-centroid characterization (Table 1). The estimated number of houses mapped within a community polygon was only 27,491; almost half of the houses in the study area occur outside of an identified community polygon.
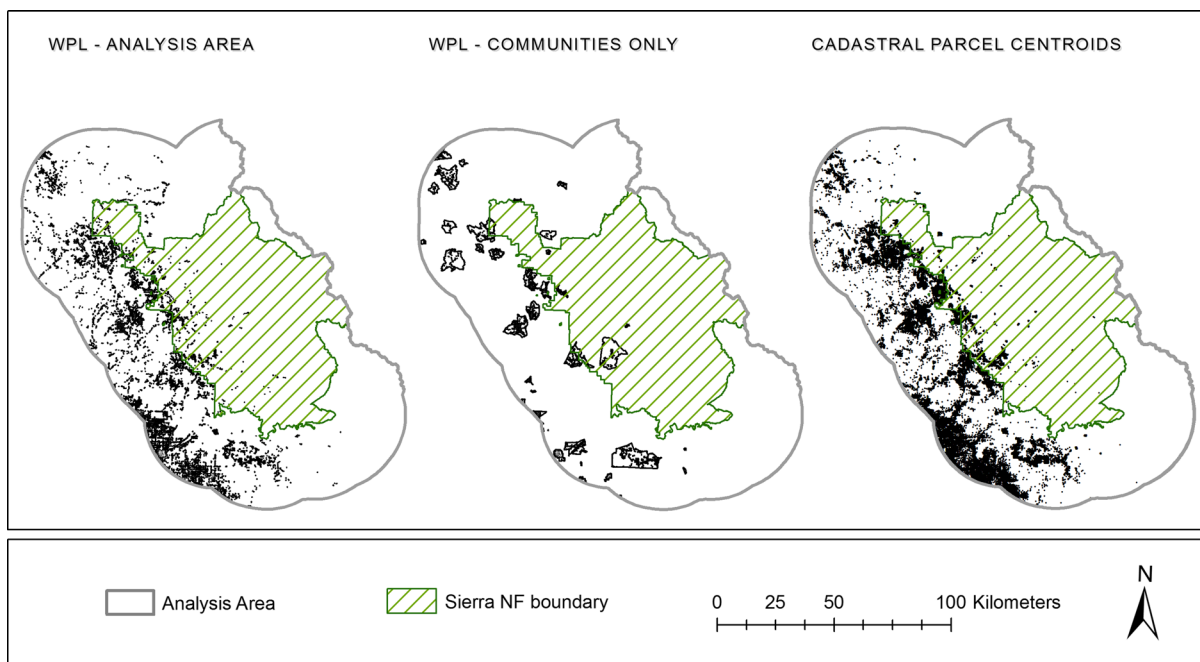
Fireshed characterization

We characterized the human-community fireshed in the study area by overlaying simulated fire perimeters with each of the three characterizations of the human community. The basic fireshed was identified as a 5-km buffer around the convex hull around the fire ignition locations that reached each of the three characterizations of a human community (Thompson et al. 2013). The 5-km buffer is included to account for uncertainty regarding whether fires starting outside the simple convex hull could actually reach the

Table 1 Summary of the estimated number of houses within the study area around the Sierra National Forest for three human community characterizations

Community characterization type	Number of houses within analysis area
WPL-analysis area	51,929
WPL-communities only	27,491
Parcel centroids	51,155

community, but simply did not in the Monte Carlo simulation. To reiterate, the basic fireshed is a simple polygon that attempts to delineate the portion of the landscape where wildfires can ignite and eventually reach a house or other highly valued resource or asset. Relative to other approaches to exposure assessment that are focused more on localized estimates of BP and/or intensity (Scott et al. 2013), the fireshed approach is focused more on capturing transmission potential from ignitions across the landscape, and delineating the spatial extent of potential sources of exposure.

To provide information about the relative propensity for fires to expose human communities to wildfire within the fireshed, we generated quantitative exposure-source information within the fireshed. To do this, we

Fig. 2 Three characterizations of the human community in the study area surrounding the Sierra National Forest

summed the number of houses occurring within each simulated fire perimeter, and then attributed those measures back to the fire's start location. For the WPL raster, we estimated the total number of houses exposed to each wildfire. For community polygons, we estimated the total number of houses within the community polygon, also based on the WPL raster. For the cadastral data, we estimated the number of improved-parcel centroids exposed to each fire.

With these three attributes now associated with the simulated fire start locations, we generated spatial exposure-source results by summarizing the mean number of houses exposed per simulated wildfire, for each measure of human community. We summarized results for ignitions occurring within sixth-level hydrologic units, the finest level available across the entire analysis area.

Results

Historical occurrence

There were 200 historical large-fire occurrences within the 2.3 million ha FOA during the period 1992–2013, for a mean of 3.93 large fires per million ha per year. Large fires represented only 1.6 % of all fires but accounted for 93 % of the area burned. Those large fires occurred on 167 large-fire days, for an average of 1.2 large fires per large-fire day. The mean annual area burned by those large fires was 12,472 ha/year. The mean large-fire size was therefore 1372 ha. The arithmetic mean of the common logarithm of historical large-fire size was 2.61, for a characteristic fire size of $10^{2.61}$, or 410 ha (Lehsten et al. 2014). A Lorenz curve for the distribution of the number of large fires against the cumulative acres burned by those fires suggests a strongly unequal distribution— the largest 20 % of the historical large fires burned roughly 80 % of the total large-fire area burned (Fig. 3). A single wildfire (the 2013 Rim Fire) accounted for 38 % of the large-fire area burned over the 22-year period. Moreover, the Rim Fire was 7.5 times larger than the next-largest fire in the historical record. Note that while we highlight the 2013 Rim Fire to illustrate large-fire potential in the FOA, the fire modeling landscape (LANDFIRE 2012) does not reflect potential changes in fuel conditions resulting from the Rim Fire.
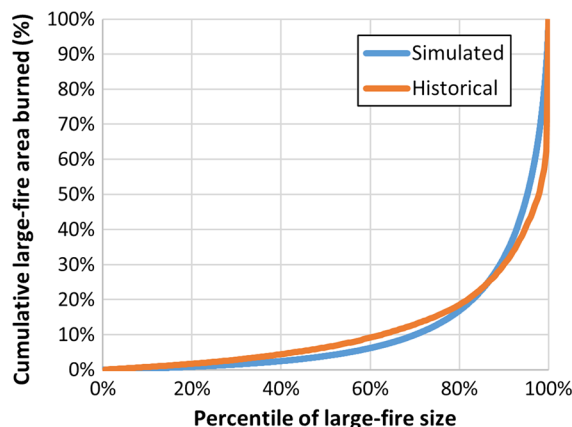
Fig. 3 Lorenz curves for historical and simulated large-fire size distributions of fires originating within the FOA. During the historical period, the smallest 80 % of fires >100 ha were responsible for only 20 % of the total large-fire area burned

Wildfire simulation

The initial simulation produced simulated fires much larger than historical. We made adjustments to the rate of spread adjustment factors for grass and shrub fuel models, and we adjusted the live fuel moisture contents in the timber-dominated fuel models to reduce fire sizes. We used a perimeter trimming factor of 2.0, which limits fire sizes more than the observed value of 2.4 for western forested landscapes (M. Finney, Research Forester, personal communication). After those adjustments, the characteristic large-fire size was still larger than historical, but further attempts to reduce the mean size were deemed too excessive, and we accepted that wildfires could indeed become much larger, on average, than occurred during the relatively short historical period. The simulated mean annual large-fire area burned was 31,273 ha/year, more than double the 22-year historical mean. The arithmetic mean large-fire size was 3432 ha, again more than double the historical mean. Finally, the characteristic large-fire size was 826 ha, once more, about double the historical size. The Lorenz curve for the simulated large-fire size distribution is very similar to the historical (Fig. 3), suggesting that FSim does a good job of simulating the fire-size distribution.

After calibration of large-fire size, we found that only 37.1 % of simulated fires reached the 100-ha large-fire threshold. Of the 167 historical large-fire days, only 98 of them (58.6 %) originated when the

ERC-G was at or above the 80th percentile. We then calculated an adjusted *AcreFract* per the equation below:

$$Acrefract_{adjusted} = 1.0 * \frac{98}{167} * \frac{80,633}{217,483} = 0.22$$

For the final simulation, we used this adjusted *AcreFract* on a 36-thread workstation, which required 74 h of computing time to simulate 10,000 fire seasons. The adjusted *AcreFract* resulted in 9.1 large fires per year, exactly equal to the historical average.

The simulated large fires were associated with the simulated fire season in which they occurred to produce exceedance probability (EP) curves for (1) the maximum large-fire size within a fire season, and (2) the total large-fire area burned during a fire season. Only about half of the iterations produced even one fire exceeding the 100 ha large-fire threshold (Fig. 5). Ten percent of the simulated fire seasons produced a larger than 33,936 ha, and 1 % of them produced a fire larger than 99,933 ha. These fire sizes represent the 10- and 100-year fire events for the FOA (Scott and Thompson 2015, Thompson et al. 2015b). The largest fire in the historical record—the 2013 Rim Fire—was 103,544 ha, the equivalent of a 105-year event. Ten percent of the fire seasons burned at least 104,960 ha, and 1 % of them burned at least 305,165 ha. The historical fire season with the greatest large-fire area burned in the period 1992 to 2013 was 2013, which burned a total of 114,008 ha, roughly equivalent to a 10-year fire season according to the simulations (by the historical record, it would be a 22-year fire season).

Burn probability (BP) varied widely across the study area (Fig. 4), with the highest BP in the productive, low-elevation forests near the western edge of the Sierra NF. The portion of the study area where the Rim Fire occurred is some of the highest probability area in the FOA. Patterns of BP outside of and along the western edge of the Sierra NF tend to vary inversely with population density (Fig. 2), suggesting lower potential for fire spread in areas with more development, and higher potential for fire spread in areas with less development and more continuous vegetation. While much of the human community footprint is located along the very low probability zones on the western edge of analysis area (odds of 1-in-200+), there are pockets of development in the intervening areas with BPs nearly an order of magnitude higher. While BP is useful for identifying human communities with the highest exposure to wildfire, the fireshed analysis provides complementary information on the spatial extent of exposure sources (see next section) (Fig. 5).
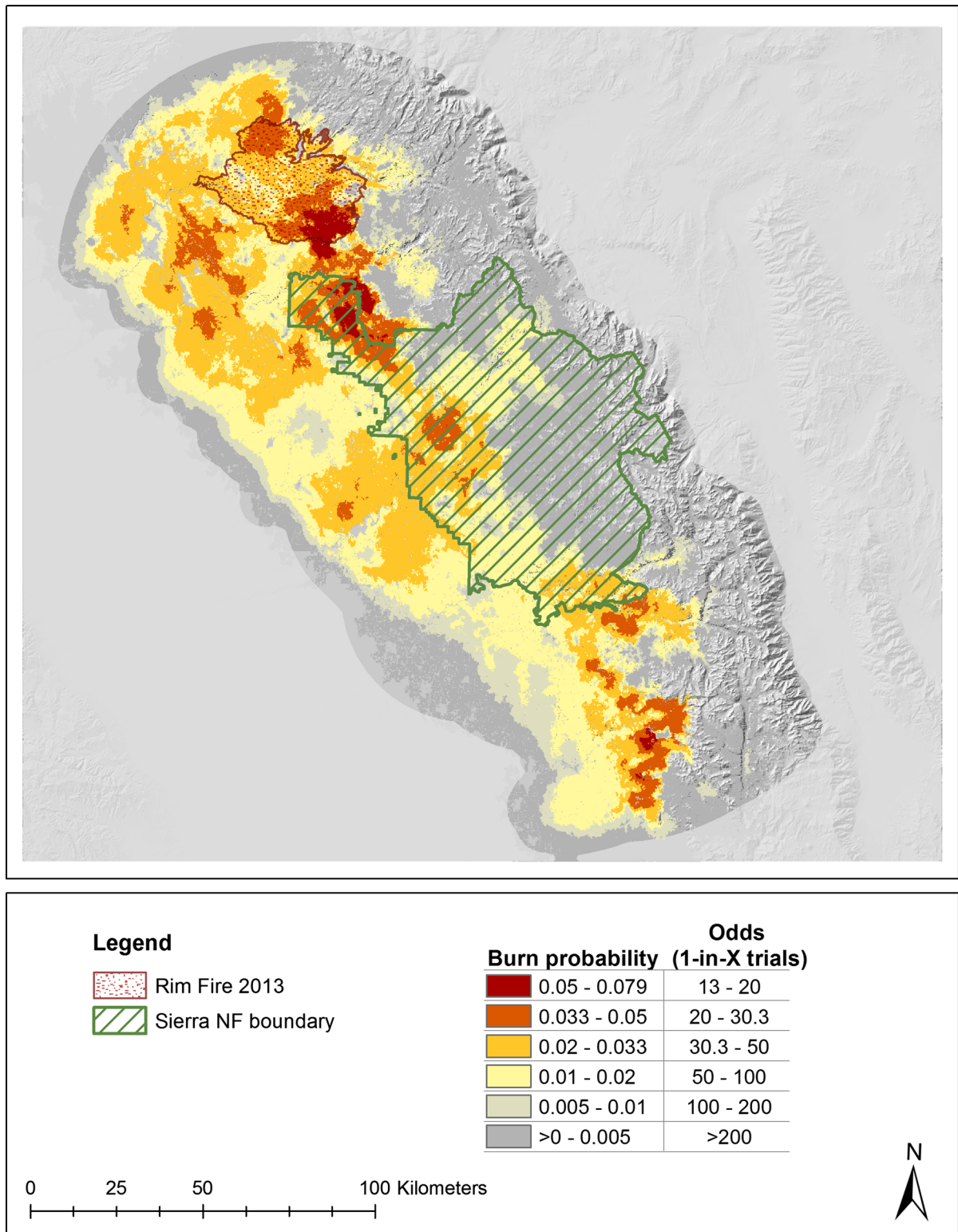
Fireshed characterization

The outer boundary of the firesheds differed slightly depending on the human community characterization type (Fig. 6). The largest fireshed (2.1 million ha) resulted from ignitions that reached any WPL pixel with a non-zero value (Table 2). Ignitions reaching parcel centroids produced the next largest fireshed at 1.9 million ha, followed by those that reached WPL pixels within a community boundary (1.6 million ha). These results follow the order of both the estimated number of houses within the analysis area and the number of ignitions reaching a "house" among the different community characterization types. The general shapes of the resulting firesheds are similar among the different human-community characterizations, with slight variations in the shape and extent due to the locations of the community polygons and parcel centroids relative to WPL (Fig. 6).
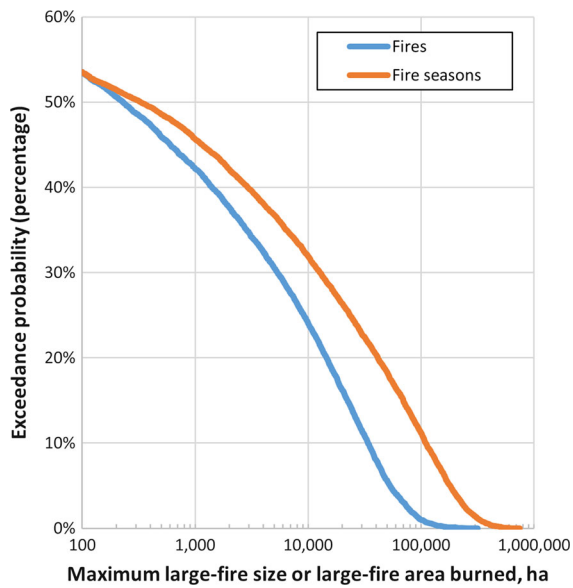
Exposure-source

Although the WPL characterization of the human community resulted in the largest fireshed, perimeter-overlay analysis of parcel centroids produced the greatest mean number of houses exposed per year (Table 2). Restricting the human community to houses within a community polygon produced a smaller fireshed, as well as a smaller number of houses exposed annually (Table 2).

Due to variability in weather and fire duration among simulated fires, not all ignitions that start in a given portion of the landscape are capable of reaching a house. All three human community characterizations produced the same pattern of exposure across the study area. The WPL and parcel centroids were very similar overall, but the WPL within community polygons showed a significantly lower mean house exposure (Fig. 6), which is consistent with the smaller number of houses represented by this dataset compared to the WPL and parcel centroids.

Legend

Rim Fire 2013

Sierra NF boundary

| Burn probability	Odds (1-in-X trials)
0.05 - 0.079	13 - 20
0.033 - 0.05	20 - 30.3
0.02 - 0.033	30.3 - 50
0.01 - 0.02	50 - 100
0.005 - 0.01	100 - 200
>0 - 0.005	>200

0   25   50   100 Kilometers

N

Fig. 4 Burn probability for simulated fires originating within the FOA

Fig. 5 Exceedance probability curves for the largest individual fire during a season and for the total area burned during a whole fire season

Exceedance probability

We generated EP curves for the number of houses exposed per fire (left panel) and per fire-season (right panel) for each community characterization type (Fig. 7). The curves for individual fires for WPL and parcel centroids are nearly identical, further indicating their representations of where houses exist are similar. The curves for WPL clipped to the community polygons indicates a lower probably of exceedance at any number of houses exposed. Both WPL and parcel centroids indicate a 45 % annual probability of at least one house, whereas the WPL-communities indicates a 32 % chance of a fire exposing at least one house. There is a 10 % chance annually that a single fire will expose at least 375 houses by WPL-communities, but in WPL for the analysis area and parcel centroids, such a 10-year event (10 % probability) would expose more than 850 and 972 houses, respectively. There is a 10 % probability of exposing at least 1518 houses during a whole fire season for WPL in the
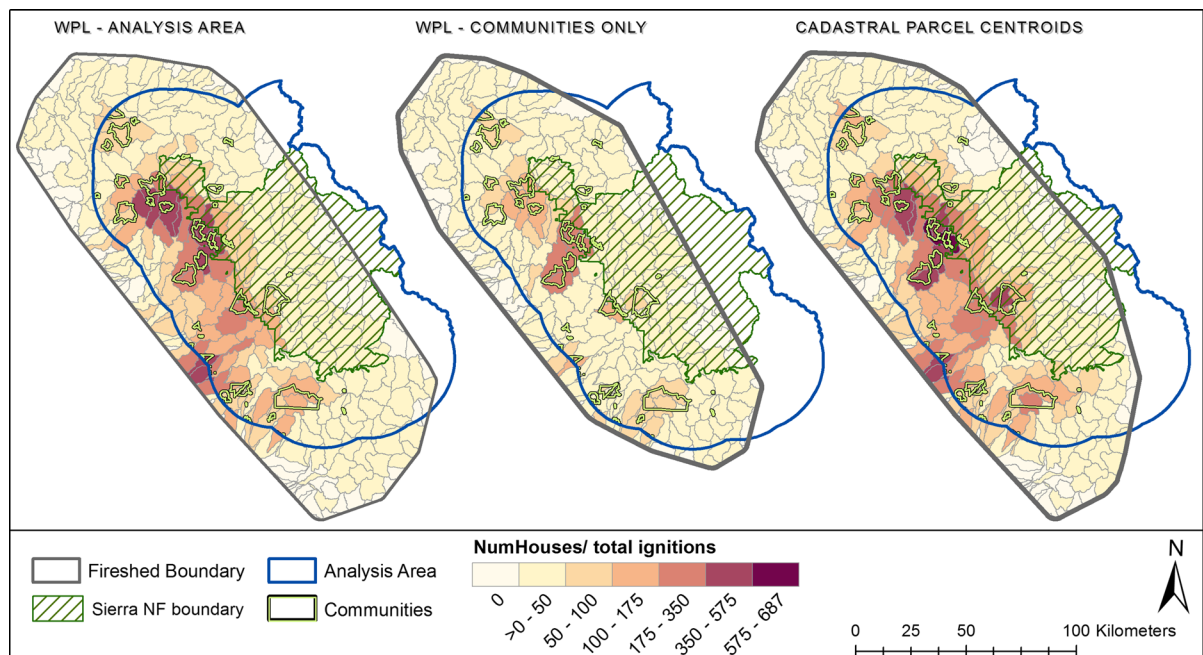
Fig. 6 Biophysical firesheds and exposure-source information for three characterizations of the human community near the Sierra National Forest

Table 2 Fireshed size and mean annual exposure to wildfire based on three characterizations of the human community near the Sierra National Forest

Community characterization type	Fireshed size (ha)	Mean number of houses exposed per year	Mean number large-fires that reaching at least one house
WPL-analysis area	2,073,650	518.7	3.78
WPL-communities only	1,628,885	195.5	1.54
Parcel centroids	1,967,611	579.9	3.32

Fig. 7 Exceedance probability curves for individual fires (*left panel*) and for whole fire seasons (*right panel*), for three different characterizations of the human community surrounding the Sierra National Forest
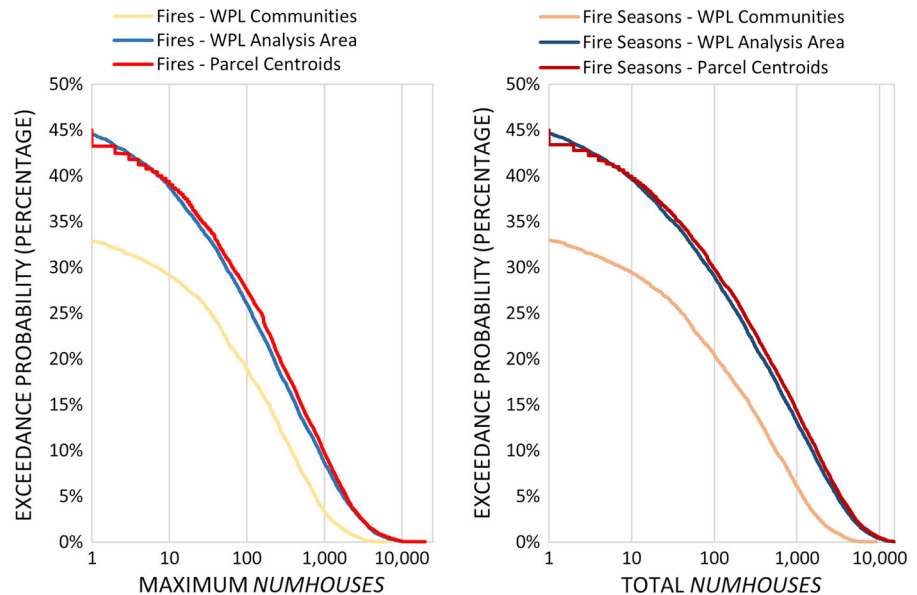
analysis area, and 1740 for parcel centroids. In contrast, there is a 10 % change of exposing at least 553 houses WPL-communities.

Comparing these results to historical data is problematic for several reasons. The Incident Status Summary report (ICS-209) has fields for tallying the number of residences threatened, damaged and destroyed. It does not tally the number of residences exposed to wildfire (within the final perimeter but not necessarily damaged or destroyed). However, the three human community characterizations we used in this analysis can be used in conjunction with an historical fire perimeter to estimate the number of houses exposed to that fire. The Rim Fire, despite its large size, exposed only 65 houses based on the WPL dataset and 111 houses based on improved-parcel centroids. The final ICS-209 for the Rim Fire dated 24 October 2013 indicated that 11 houses were destroyed, 10–17 % of the houses exposed. This number of houses exposed in a single fire has a 0.27–0.29 annual

probability of exceedance for WPL and parcel centroids respectively, making the Rim Fire equivalent to a 3.5- to 4-year event in terms of houses exposed, even though it was a 105-year event in terms of area burned.

Discussion

Biophysical fireshed analysis results revealed notable similarities and differences across the three human community characterization approaches. Point-based and raster-based methods yielded nearly identical results in terms of our three primary metrics (Table 2), spatial patterns of exposure sources (Fig. 6), and house exposure probabilities (Fig. 7). The polygon-based method by contrast resulted in a very different characterization of the fireshed and lower estimates for house exposure. Restricting the characterization of where the houses are to a polygon

representing census-designated places eliminated almost half of the houses from the analysis. For this specific case study, community polygons are inadequate representations of where houses actually exist across a large landscape.

That mapping human communities with a smaller collective footprint would lead to lower exposure levels might appear self-evident, but carries significant implications. First, the magnitude of the problem might be understated, leading to insufficient investments of time and resources in mitigation. Second, prioritization of exposure sources on the landscape might be targeting the wrong areas, limiting the effectiveness and efficiency of mitigation measures like fuel treatments. This latter point is particularly noticeable in Fig. 6, where the identification of sources of ignitions that reach homes is highly variable across the mapping methods. Using the polygon approach, planning efforts might fail to consider investing in mitigation within a high risk-source area along the southwestern flank of the fireshed.

Ager et al. (2015) caution that the scale of community wildfire protection planning is often mismatched with the scale of landscape risk analysis. Our findings build from this critique and highlight the importance of identifying the correct scale for landscape risk analysis. While analysis of potential wildfire threats to community boundaries likely provides utility for a variety of planning purposes (e.g., for local agencies and fire districts), it may come at the expense of identifying more socially optimal mitigation investments if analyses do not also consider a more comprehensive representation of house locations. We should note that this critique speaks only to the biophysical dimensions of fireshed planning, and not to social issues related to capacity, collaboration, communication, or education. Our point is that it is important to have a complete and accurate understanding of landscape scale exposure and risk transmission before deciding the scale at which collaborative planning and co-management of risk will take place.

Our analysis is strategic rather than tactical in nature, intended to provide a "big picture" overview of human community exposure to wildfire. The methods we developed could be used at a finer scale, and our analysis suggests two things to support that work: (1) which communities should receive the first such attention; and (2) which characterization of the

human community may be most appropriate for that finer-scale analysis. At the broader scale, our analysis can help identify which areas and landowners comprise the greatest exposure sources, and whether options like hazardous fuel reduction treatments are appropriate and feasible in these areas. For instance, Fig. 6 indicates that most sources of exposure lie outside the boundary of the Sierra NF, suggesting that fuel treatments on the federal estate alone may not be likely to significantly reduce human community exposure and risk. Accurately characterizing the nature of the problem is a critical first step in mitigation efforts, and the fireshed analysis provides richer information on sources of exposure relative to focusing on localized exposure using only BP outputs.

However, our analysis also reveals some limitations of the biophysical fireshed concept. If we were to change the size, shape, or location of the fire modeling landscape, it is possible that we would change the extent of mapped human communities, leading to different spatial characterizations of firesheds and exposure sources. This issue is likely more problematic as population is more continuously connected in fire-prone areas, for instance the Front Range of Colorado, USA. In such cases a stronger focus on identifying exposure and risk sources is likely more useful than the actual size and shape of the fireshed itself. The ratios of the number of houses exposed per total ignitions within a watershed (Fig. 6) could therefore offer more readily actionable information for mitigation planning. This summarization approach is similar to other fireshed-related work characterizing exposure sources according to the distance from the resource or asset of interest (Thompson et al. 2013). The fireshed approach likely still has great utility however for other resources and assets with more readily definable boundaries, such as municipal watersheds and critical infrastructure.

Future work could begin by applying similar exposure source methods to other landscapes, and seeing if similar relationships between human community characterization hold. WPL is available for 17 western states (Oregon Department of Forestry 2013), parcel data is available for approximately 70 % of the United States (Calkin et al. 2011), and a raster dataset similar to WPL is available nationwide (Haas et al. 2013). Analysis could actually identify risk sources by incorporating susceptibility to fire (Thompson et al. 2015b; Scott and Thompson 2015). Additional

analysis could explore how the size and shape of firesheds change seasonally and under alternative fire and fuel management scenarios.

Compliance with ethical standards

Conflict of interest None.

Human and animal rights This article does not contain any studies with human or animal subjects.

References

Ager, A. A., Day, M. A., Finney, M. A., Vance-Borland, K., & Vaillant, N. M. (2014a). Analyzing the transmission of wildfire exposure on a fire-prone landscape in Oregon, USA. *Forest Ecology and Management, 334*(15 December 2014), 377–390.

Ager, A. A., Day, M. A., McHugh, C. W., Short, K., Gilbertson-Day, J., Finney, M. A., et al. (2014b). Wildfire exposure and fuel management on western US national forests. *Journal of Environmental Management, 145*(1 December 2014), 54–70.

Ager, A. A., Kline, J. D., & Fischer, A. P. (2015). Coupling the biophysical and social dimensions of wildfire risk to improve wildfire mitigation planning. *Risk Analysis, 35*(8), 1393–1406.

Alcasena, F., Salis, M., Ager, A., Arca, B., Molina, D., & Spano, D. (2015). Assessing Landscape Scale wildfire exposure for highly valued resources in a Mediterranean area. *Environmental Management, 55*(5), 1200–1216.

Calkin, D. E., Cohen, J. D., Finney, M. A., & Thompson, M. P. (2014). How risk management can prevent future wildfire disasters in the wildland–urban interface. *Proceedings of the National Academy of Sciences, 111*(2), 746–751.

Calkin, D. E., Rieck, J. D., Hyde, K. D., & Kaiden, J. D. (2011). Built structure identification in wildland fire decision support. *International Journal of Wildland Fire, 20*(1), 78–90.

Cova, T. J., Theobald, D. M., Norman, J. B, I. I. I., & Siebeneck, L. K. (2013). Mapping wildfire evacuation vulnerability in the western US: The limits of infrastructure. *GeoJournal, 78*(2), 273–285.

Dennison, P. E., Cova, T. J., & Mortiz, M. A. (2007). WUIVAC: A wildland–urban interface evacuation trigger model applied in strategic wildfire scenarios. *Natural Hazards, 41*(1), 181–199.

Finney, M. A. (1998). *FARSITE: Fire area simulator—Model development and evaluation. Research paper RMRS-RP-4*. Fort Collins: U.S. Department of Agriculture, Forest Service, Rocky Mountain Research Station.

Finney, M. A. (2002). Fire growth using minimum travel time methods. *Canadian Journal of Forest Research, 32*(8), 1420–1424.

Finney, M. A., McHugh, C. W., Grenfell, I. C., Riley, K. L., & Short, K. C. (2011). A simulation of probabilistic wildfire risk components for the continental United States. *Stochastic Environmental Research and Risk Assessment, 25*(7), 973–1000.

Haas, J. R., Calkin, D. E., & Thompson, M. P. (2013). A national approach for integrating wildfire simulation modeling into Wildland Urban Interface risk assessments within the United States. *Landscape and Urban Planning, 119*(November 2013), 44–53.

Haas, J. R., Calkin, D. E., & Thompson, M. P. (2015). Wildfire risk transmission in the Colorado Front Range, USA. *Risk Analysis, 35*(2), 226–240.

Kalabokidis, K., Palaiologou, P., Gerasopoulos, E., Giannakopoulos, C., Kostopoulou, E., & Zerefos, C. (2015). Effect of climate change projections on forest fire behavior and values-at-risk in Southwestern Greece. *Forests, 6*(6), 2214.

Lehsten, V., de Groot, W. J., Flannigan, M., George, C., Harmand, P., & Balzter, H. (2014). Wildfires in boreal ecoregions: Evaluating the power law assumption and intra-annual and interannual variations. *Journal of Geophysical Research: Biogeosciences, 119*(1), 14–23.

Mitsopoulos, I., Mallinis, G., & Arianoutsou, M. (2015). Wildfire risk assessment in a typical Mediterranean wildland–urban interface of Greece. *Environmental Management, 55*(4), 900–915.

Moritz, M. A., Batllori, E., Bradstock, R. A., Gill, A. M., Handmer, J., Hessburg, P. F., et al. (2014). Learning to coexist with wildfire. *Nature, 515*(7525), 58–66.

Oregon Department of Forestry, Western Forestry Leadership Coalition, and Council of Western State Foresters. (2013). *Westwide wildfire risk assessment final report*. Salem: Oregon Department of Forestry. http://www.odf.state.or.us/gis/data/Fire/West_Wide_Assessment/WWA_Final Report.pdf. Accessed June 24, 2015.

Pacheco, A. P., Claro, J., Fernandes, P. M., de Neufville, R., Oliveira, T. M., Borges, J. G., et al. (2015). Cohesive fire management within an uncertain environment: A review of risk handling and decision support systems. *Forest Ecology and Management, 347*(1 July 2015), 1–17.

Radeloff, V. C., Hammer, R. B., Stewart, S. I., Fried, J. S., Holcomb, S. S., & McKeefry, J. F. (2005). The wildland–urban interface in the United States. *Ecological Applications, 15*(3), 799–805.

Ryan, K. C., & Opperman, T. S. (2013). LANDFIRE–A national vegetation/fuels data base for use in fuels treatment, restoration, and suppression planning. *Forest Ecology and Management, 294*(15 April 2013), 208–216.

Scott, J. H., & Burgan, R. E. (2005). *Standard fire behavior fuel models: A comprehensive set for use with Rothermel's surface fire spread model* (p. 72). Fort Collins: USDA Forest Service, Rocky Mountain Research Station, General Technical Report RMRS-GTR-153.

Scott, J. H., & Reinhardt, E. (2001). *Assessing crown fire potential by linking models of surface and crown fire behavior. Research Paper RMRS-RP-29* (p. 56). Fort Collins: U.S. Department of Agriculture, Forest Service, Rocky Mountain Research Station.

Scott, J., Helmbrecht, D., Parks, S., & Miller, C. (2012). Quantifying the threat of unsuppressed wildfires reaching

the adjacent wildland–urban interface on the Bridger-Teton National Forest, Wyoming, USA. *Fire Ecology, 8*(2), 125–142.

Scott, J. H., & Thompson, M. P. (2015). Emerging concepts in wildfire risk assessment and management. In *Proceedings of the large-fire conference; Missoula, Montana; May 2014. Proc. RMRS-P-73*. Fort Collins: U.S. Department of Agriculture, Forest Service, Rocky Mountain Research Station.

Scott, J. H., Thompson, M. P. & Calkin, D. E. (2013). A wildfire risk assessment framework for land and resource management. In *Gen. Tech. Rep. RMRS-GTR-315*. U.S. Department of Agriculture, Forest Service, Rocky Mountain Research Station.

Short, K. C. (2014). *Spatial wildfire occurrence data for the United States, 1992–2012 [FPA_FOD_20140428]* (2nd ed.). Fort Collins: Forest Service Research Data Archive.

Strauss, D., Bender, L., & Mees, R. (1989). Do one percent of forest fires cause ninety-nine percent of the damage? *Forest Science, 35*(2), 319–328.

Thompson, M. P., & Calkin, D. E. (2011). Uncertainty and risk in wildland fire management: A review. *Journal of Environmental Management, 92*(8), 1895–1909.

Thompson, M. P., Gilbertson-Day, J. W. & Scott, J. H. (2015b). Integrating pixel-and polygon-based approaches to wildfire risk assessment: Application to a high-value watershed on the Pike and San Isabel National Forests, Colorado, USA. *Environmental Modeling & Assessment*, 1–15. doi:10.1007/s10666-015-9469-z.

Thompson, M. P., Haas, J. R., Gilbertson-Day, J. W., Scott, J. H., Langowski, P., Bowne, E., et al. (2015a). Development and application of a geospatial wildfire exposure and risk calculation tool. *Environmental Modelling and Software, 63*(January 2015), 61–72.

Thompson, M. P., Scott, J., Kaiden, J. D., & Gilbertson-Day, J. W. (2013). A polygon-based modeling approach to assess exposure of resources and assets to wildfire. *Natural Hazards, 67*(2), 627–644.

U.S. Census. (2014). Cartographic Boundary Shapefiles—Places (Incorporated Places and Census Designated Places). https://www.census.gov/geo/maps-data/data/cbf/cbf_place.html. Accessed May 26, 2015.

Williams, J. (2013). Exploring the onset of high-impact megafires through a forest land management prism. *Forest Ecology and Management, 294*(15 April 2013), 4–10.

Williams, D. R., Jakes, P. J., Burns, S., Cheng, A. S., Nelson, K. C., Sturtevant, V., et al. (2012). Community wildfire protection planning: The importance of framing, scale, and building sustainable capacity. *Journal of Forestry, 110*(8), 415–420.